

Development of single-filter Doppler signal discrimination method for incoherent Doppler lidar system

SUNGCHUL CHOI¹, SUNGHOON BAIK¹, SEUNGKYU PARK¹, IMKANG SONG², DUKHYEON KIM^{3*}, JINMAN JUNG¹

¹Laboratory for Quantum Optics, Korea Atomic Energy Research Institute (KAERI), Daedeok-Daero 989-111, Yuseong-Gu, Daejeon 305-353, Korea

²Department of Physics, Kongju National University, 182 Singwan-Dong, Gongju, Chungnam 314-701, Korea

³Division of Cultural Studies, Hanbat National University, 16-1 Duckmyoung-Dong, Yuseong-Gu, Daejeon 305-719, Korea

*Corresponding author: dhkim7575@paran.com

In this paper, we present a single-filter Doppler signal discrimination method for an incoherent Doppler lidar system that has been developed by the Korea Atomic Energy Research Institute. For the incoherent Doppler system, we use an injection-seeded pulsed Nd:YAG laser as a transmitter and an iodine filter as a Doppler frequency discriminator. To reduce the temperature-dependence error, a single iodine filter is used to lock the laser frequency and to detect the Doppler frequency shift. The mean squared error of the frequency locking process is 3.87 MHz, which corresponds to a wind velocity detection limit of approximately 1.04 m/s. The range and velocity measurements are performed using a tunable rotating disc. The results are consistent with those of previous studies in terms of the correlation between the signal ratio (signal/reference) and the actual speed of the rotating disc.

Keywords: injection-seeded laser, lidar, frequency locking, incoherent Doppler.

1. Introduction

The use of lidar technology to measure atmospheric winds has gained importance in atmospheric dynamics and weather forecasting based on numerical models [1]. Three-dimensional wind measurements, which are required to be well resolved in space and range, have been performed to show the efficacy of the Doppler wind lidar [2, 3].

Some researchers have classified Doppler wind lidars into two categories: coherent Doppler lidar and incoherent (direct detection) Doppler lidar [4–7]. Coherent Doppler lidar systems use a heterodyning technique to measure atmospheric winds. Most

coherent Doppler lidar techniques depend on Mie scattering from aerosols. Their narrow bandwidth permits the suppression of background noise by heterodyning with a local oscillator, resulting in shot-noise limited detection. Although coherent Doppler lidar has a high spectral resolution, it suffers from certain drawbacks because of the system coherence length, requisite high-quality optics, and low scattering coefficient. Recently, incoherent (direct detection) Doppler lidar has gained popularity because of the rapid development of optoelectronic techniques. For lower atmosphere wind measurements, LIU *et al.* proposed the use of an iodine edge Doppler filter for spectral analysis of backscattered light from both molecules and aerosols [8]. Further, the Doppler lidar based on an iodine filter has two advantages in this application. First, such a metal vapor filter has absolute frequency calibration, and it is repeatable from day to day and from location to location, unlike an etalon system. Second, this filter has several absorption lines near 532 nm, which falls within the reach of a tunable frequency-doubled Nd:YAG laser.

In this study, we investigate a Doppler signal discrimination system for developing incoherent Doppler lidar using an iodine absorption filter. We apply incoherent Doppler wavelength discrimination to the Doppler lidar receiving system and evaluate the system's performance using a rotating disc.

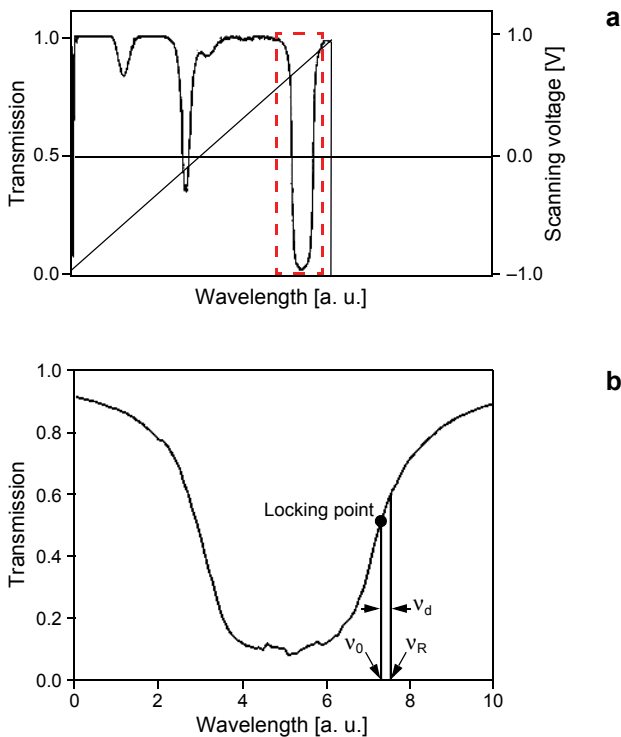


Fig. 1. Plots of iodine transmission ratio against tunable seeder laser wavelength for external input voltage of -1 V to $+1$ V, which is varied in steps of $100 \mu\text{V}$ (a). Laser output at 532 nm is locked to the halfway point on the edge of the iodine spectral absorption line (b).

2. Measurement theory

For incoherent Doppler lidar measurements, the absorption profile of the molecular iodine filter must be both stable and known. Figure 1a shows a plot of the iodine transmission ratio against the tunable seeder laser wavelength at an external input voltage of -1 V to $+1$ V, which is varied in steps of $100 \mu\text{V}$; corresponding to 0.87 MHz. Figure 1b shows a plot of the iodine transmission ratio against a wavelength of approximately 532 nm, which is where the laser is locked to the halfway point on the edge of the iodine spectral absorption line to stabilize the frequency. This indicates that because of Doppler effects, a slight variation in the wavelength is reflected by a large change in the magnitude of transmission. Figure 2 shows the transmission ratio of a Fabry–Pérot etalon with a known free spectral range (FSR) of 4 GHz. The transmission ratio of the Fabry–Pérot etalon is determined by varying the frequency control input voltage from -1 V to $+1$ V in steps of $100 \mu\text{V}$; corresponding to 0.87 MHz.

3. Experiment and results

The following three factors must be taken into account to design an incoherent Doppler lidar system: *i*) the laser bandwidth, *ii*) a laser frequency locking system, and *iii*) an edge filter. In particular, the laser bandwidth should be narrow enough to detect even a small Doppler-shifted wavelength change, the laser frequency should not be changed by more than the minimum Doppler frequency, and the iodine filter should be able to detect a small Doppler shift in frequency.

Table 1 lists the major system parameters, whereas Fig. 3 shows the schematic diagram for the transmitting and receiving systems. The transmitter comprises a tunable, cw single-frequency Nd:YVO₄ seeder laser (Model 6350, Spectra-Physics) and a commercial Q-switched Nd:YAG pulsed laser, which is equipped with electronics

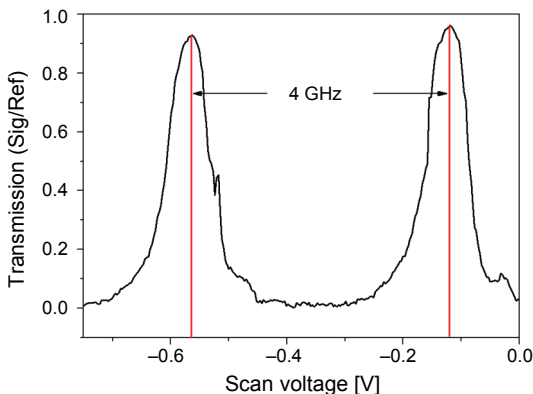


Fig. 2. Transmission ratio of Fabry–Pérot etalon with known free spectral range (FSR) of 4 GHz. This transmission ratio is measured by varying the frequency control input voltage from -1 V to $+1$ V in steps of $100 \mu\text{V}$.

T a b l e 1. Major system parameters of incoherent Doppler lidar system.

	Parameter	Specification
Etalon	Free spectral range	4 GHz
	Effective finesse	12
	Surface flatness	$\lambda/100$
	Refractive index	1.467
Laser	Seeder laser linewidth	<10 kHz
	Bandwidth	100 MHz
	Type	Nd:YAG
Data acquisition	USB-6211(National Instruments DAQ card)	

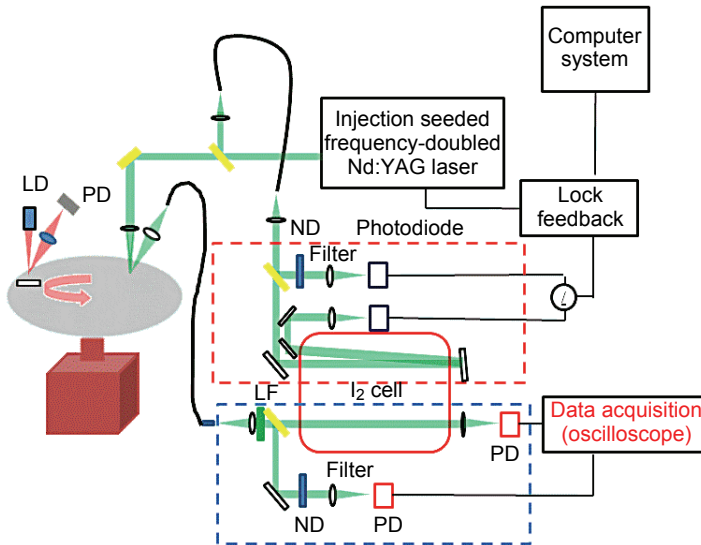


Fig. 3. Schematic diagram of the transmitting and receiving systems. A single iodine filter is used to lock the transmitter laser frequency and detect the Doppler frequency shift.

to reduce the Q-switch build-up time and trigger a laser pulse. The output wavelength of the seeder laser is approximately $1.064 \mu\text{m}$.

We divide the injection-seeded laser beam into two separate beams by using a beam splitter (T70:R30). The transmitted beam (T70) is sent to a rotating disc, whereas the reflected beam (R30) is transmitted to a frequency locking processor through an optical fiber. The laser light is scattered from the rotating disc with an adjustable speed, as shown in Fig. 3. The speed of the rotating disc can be determined from the Doppler receiving system and an improvised encoder, which is installed on the rotating disc using a He-Ne laser. The Doppler-shifted scattered light is collected in the backward direction and is transmitted through the optical fiber. Subsequently, the light is divided into two channels. One (reference) channel detects the scattered

light directly, whereas the other channel detects the filtered light that passes through an iodine cell of 20 cm in length. Each channel is monitored by a different photodiode.

If the backscattered light frequency is ν_R , the Doppler frequency shift is given by $\nu_D = \nu_0 - \nu_R$. Moreover, this Doppler frequency shift can be expressed as follows [8]:

$$\nu_D = 2 \frac{V_R}{\lambda} \quad (1)$$

where λ is the laser wavelength and V_R is the forward radial velocity of the scatter. If $h(\nu)$ is the spectral distribution of the normalized laser energy, the normalized transmission function $F(\nu)$ is defined as follows:

$$F(\nu_0) = \int_{-\infty}^{+\infty} h(\nu_0 - \nu') F(\nu') d\nu' \quad (2)$$

where ν_0 is the locked frequency. This normalized transmission function $F(\nu)$ can be plotted against the radial velocity relative to the locked frequency point. The speed can be determined by comparing the normalized transmission function $F(\nu)$ with the experimentally measured ratio of backscattered light, $R(\nu) = N(\nu)/2N_0$, where $N(\nu)$ and N_0 are the backscattered light of the measurement and reference channels, respectively. The relative efficiencies of the two channels are such that each channel detects an identical amount of signal from a fixed target, and thus, $F(0) = 0.5$. The Doppler shift due to a moving scatter is given as follows

$$\nu_D = 2 \frac{V_R}{\lambda} = \frac{\Delta F(\nu)}{\partial F(\nu)/\partial \nu} = \frac{\Delta R(\nu)}{\partial F(\nu)/\partial \nu} \quad (3)$$

3.1. Injection-seeded laser

The Doppler frequency shift that corresponds to a 1 m/s line-of-sight wind speed is 3.76 MHz when the laser is Nd:YAG second harmonic (532 nm). Without an injection-seeded laser, the bandwidth or linewidth of the current laser is approximately 60 GHz. It is impossible to measure the Doppler-shifted wavelength with this type of Nd:YAG laser. An injection-seeded laser is required to obtain a narrow linewidth from the pulsed laser. We used the single longitudinal mode of a cw seeder laser as the injection source, with a bandwidth of less than 10 kHz. Consequently, we obtained a pulsed laser with a bandwidth of 100 MHz at 532 nm.

3.2. Frequency locking process

For measuring the Doppler-shifted wavelength, the spectral absorption profile of the molecular iodine filter must be known. In the case of incoherent Doppler lidar, temperature control of the iodine vapor filter is one of the most important issues because the spectral absorption profiles of the iodine vapor depend on pressure and

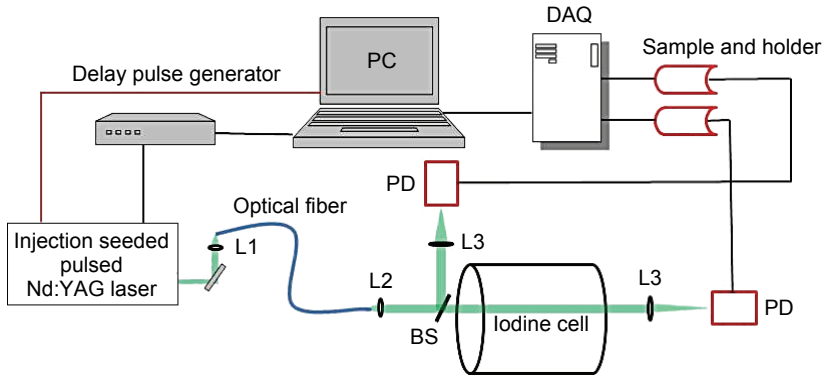


Fig. 4. Schematic diagram of laser frequency locking.

temperature. To reduce the temperature-dependence error, a single iodine filter is used to lock the laser frequency and to detect the Doppler frequency shift. To permit its use as the absolute frequency reference, the temperature of the iodine cell is maintained at 65 °C (within 0.01 °C rms), whereas the temperature of its cell body is maintained at 70 °C (within 0.1 °C rms).

The optical diagram of frequency locking is shown in Fig. 4. We divide the light using a beam splitter (T70:R30) before transmitting it to the rotating disc. After collection, the backscattered light is collimated and transmitted through the optical fiber via lenses (L1, L2). The collimated light is divided using a beam splitter (T50:R50). One path is used for monitoring the frequency shift, and the other path is used for monitoring energy. When the backscattered light is frequency shifted, the variation in the laser energy through the iodine filter can be detected from the two optical paths. Then, the output of the reference channel is transmitted to a computer as the proportional feedback signal. Signals from the two photodiodes are sampled using a National Instruments DAQ card (USB-6211) in a computer. For decreasing signal fluctuation, a sample-and-hold device (LF 398) is used before the signal is transmitted through the DAQ device. In addition, the DAQ device transmits the DC voltage feedback signal to the seeder laser for frequency stabilization. The step voltage is approximately 100 μ V, and the adjustable seeder laser frequency is approximately 0.87 MHz. To measure the width of the iodine absorption line, we used a Fabry–Pérot etalon that has an FSR of 4 GHz.

Figure 5a shows the stability of the laser frequency after locking. The mean squared error of the signal ratio (signal/reference) is 0.0066 (3.83 MHz), which corresponds to a wind velocity of approximately 1.04 m/s. To reduce the time resolution of the locking process, the input voltage is set for a signal ratio of 0.5. To verify the locking process, the iodine cell shown in Fig. 4 is replaced with a Fabry–Pérot etalon.

Figure 5b shows the result for the seeder laser using the Fabry–Pérot etalon. The mean squared error of the signal ratio (signal/reference) is 0.0049 (4.44 MHz),

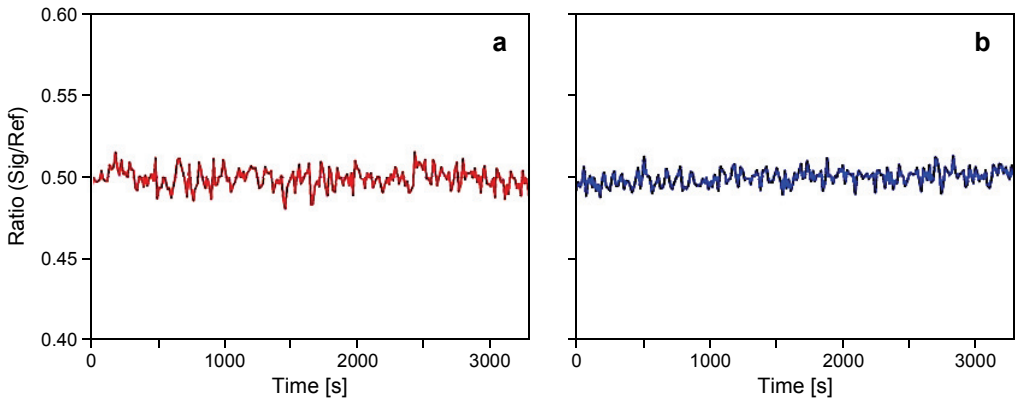


Fig. 5. Stability of laser frequency locking for iodine absorption line (a) and Fabry-Pérot etalon (b).

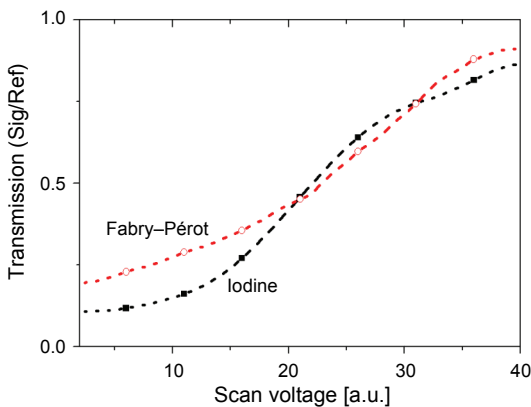


Fig. 6. Transmission ratios of iodine absorption and Fabry-Pérot etalon. The curve for iodine shows a steeper slope than that for the Fabry-Pérot etalon.

which corresponds to a wind velocity of approximately 1.2 m/s. In fact, for a transmission ratio of approximately 0.5, a change in the input voltage of the seeder laser controller results in a difference in the slope between the transmission curves of the two filters. This indicates that the iodine curve has a sharper edge, as can be observed in Fig. 6.

3.3. Doppler frequency discrimination system

To test our metal receiving system, we used an electrical motor to drive a rotating disc as a moving object, as shown in Fig. 3. The surface of the disc edge is covered with a white paper that can diffuse the incident laser light that is transmitted to the disc along the direction of its surface. All measurements are averaged over 500 pulses. The scattered light is collected in the backward direction and is transmitted through the optical fiber.

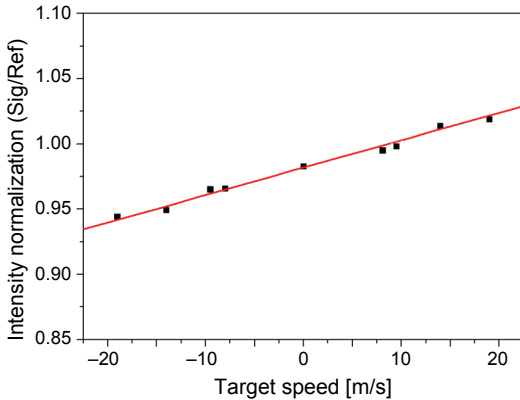


Fig. 7. Plot of changes in the transmitted signal against the actual speed of the rotating disc.

During data acquisition, we monitored the frequency locking point to determine the variation in laser frequency. The standard deviation of the locking frequency for a duration of 4 h was below 4 MHz, which corresponded to a velocity uncertainty of 1.08 m/s. Figure 7 shows a plot of the changes in the transmitted signal against the actual speed of the rotating disc. The measured standard deviation for each data point is 3.94 MHz, which corresponds to a velocity of approximately 1.06 m/s. The results indicate that the correlation between the signal ratio (signal/reference) and the actual speed of the rotating disc is consistent with that found in previous studies [8, 9].

4. Conclusions

In this paper, we presented the development of a single-filter Doppler signal discrimination method for an incoherent Doppler lidar system developed by the Korea Atomic Research Institute. For the Doppler lidar system, we used an injection-seeded pulsed Nd:YAG laser as the transmitter and an iodine filter as the Doppler frequency discriminator. Using the improvised Doppler frequency discriminator, we obtained a Doppler signal with a high spectral resolution and a wide field of view, even with low optical adjustable mechanics. The velocity measurements were performed using a tunable rotating disc. The measured standard deviation for each data point was 3.94 MHz, which corresponds to a velocity of approximately 1.06 m/s. This value (1.06 m/s) is similar to other incoherent Doppler lidar detection limits [10–12]. The results indicate that the correlation between the signal ratio (signal/reference) and the actual speed of the rotating disc is consistent with that of previous studies. In the future, we plan to perform atmospheric measurements.

Acknowledgements – This work was funded by the Korea Meteorological Administration Research and Development Program under grant CATER 2006-3101.

References

- [1] MENZIES R.T., *Doppler lidar atmospheric wind sensor: A comparative performance evaluation for global measurement application from earth orbit*, *Applied Optics* **25**(15), 1986, pp. 2546–2553.
- [2] REES D., McDERMID I.S., *Doppler lidar atmospheric wind sensor: Reevaluation of a 355-nm incoherent Doppler lidar*, *Applied Optics* **29**(28), 1990, pp. 4133–4144.
- [3] MCGILL M.J., SKINNER W.R., IRGANG T.D., *Validation of wind profiles measured with incoherent Doppler lidar*, *Applied Optics* **36**(9), 1997, pp. 1928–1932.
- [4] FRIEDMAN J.S., TEPLEY C.A., CASTLEBERG P.A., ROE H., *Middle-atmospheric Doppler lidar using an iodine-vapor edge filter*, *Optics Letters* **22**(21), 1997, pp. 1648–1650.
- [5] MCKAY J.A., *Assessment of a multibeam Fizeau wedge interferometer for Doppler wind lidar*, *Applied Optics* **41**(9), 2002, pp. 1760–1767.
- [6] CHIAO-YAO SHE, JIA YUE, ZHAO-AI YAN, HAIR J.W., JIN-JIA GUO, SONG-HUA WU, ZHI-SHEN LIU, *Direct-detection Doppler wind measurements with a Cabannes–Mie lidar: A. Comparison between iodine vapor filter and Fabry–Perot interferometer methods*, *Applied Optics* **46**(20), 2007, pp. 4434–4443.
- [7] CHIAO-YAO SHE, JIA YUE, ZHAO-AI YAN, HAIR J.W., JIN-JIA GUO, SONG-HUA WU, ZHI-SHEN LIU, *Direct-detection Doppler wind measurements with a Cabannes–Mie lidar: B. Impact of aerosol variation on iodine vapor filter methods*, *Applied Optics* **46**(20), 2007, pp. 4444–4454.
- [8] LIU Z.S., CHEN W.B., ZHANG T.L., HAIR J.W., SHE C.Y., *An incoherent Doppler lidar for ground-based atmospheric wind profiling*, *Applied Physics B* **64**(5), 1997, pp. 561–566.
- [9] DUKHYEON KIM, SEONGKOK KWON, HYUNGKI CHA, YOUNGGI KIM, JEONGHAEI SUNWOO, *A newly designed single etalon double edge Doppler wind lidar receiving optical system*, *Review of Scientific Instruments* **79**(12), 2008, article 123111.
- [10] SHIBATA Y., NAGASAWA C., ABO M., NAGAI T., *Low-altitude wind measurement using incoherent Doppler lidar by utilizing both absorption slopes of the iodine absorption spectrum*, *Japanese Journal of Applied Physics* **48**, 2009, article 126501.
- [11] SHIBATA Y., NAGASAWA C., ABO M., NAGAI T., *System evaluation of an incoherent wind Doppler LIDAR using an iodine filter*, *Japanese Journal of Applied Physics* **48**, 2009, article 032401.
- [12] ZHI-SHEN LIU, BING-YI LIU, SONG-HUA WU, ZHI-GANG LI, ZHANG-JUN WANG, *High spatial and temporal resolution mobile incoherent Doppler lidar for sea surface wind measurements*, *Optics Letters* **33**(13), 2008, pp. 1485–1487.

*Received September 26, 2011
in revised form January 9, 2012*